

Object Detection and Heading Forecasting by fusing Raw Radar Data using Cross Attention

Ravi Kothari¹, Ali Kariminezhad¹, Christian Mayr¹, Haoming Zhang²

Abstract—Radar has been believed to be an inevitable sensor for advanced driver assistance systems (ADAS) for decades. Along with providing robust range, angle and velocity measurements, it is also cost-effective. Hence, radar is expected to play a big role in the next generation ADAS.

In this paper, we propose a neural network for object detection and heading forecasting based on radar by fusing three raw radar channels with a cross-attention mechanism. We also introduce an improved ground truth augmentation method based on Bivariate norm, which represents the object labels in a more realistic form for radar measurements. Our results show 5% better mAP compared to state-of-the-art methods. To the best of our knowledge, this is the first attempt in the radar field, where cross-attention is utilized for object detection and heading forecasting without the use of object tracking and association.

Index Terms—DNN, cross-attention, raw radar data, object detection, heading forecasting

I. INTRODUCTION

The number of vehicles with advanced driver assistance is rising rapidly. In Europe alone more than 8% of the new car sale (Q2, 2019) were equipped with level 2 ADAS [1]. Furthermore, the consumer demands for safety and autonomy are driving the next generation ADAS to handle complex scenarios such as urban and night driving. With the presence of a vehicle in an environment with vulnerable road users (VRU's), the sensor suite must be robust. Cameras have been highly believed to be the main sources of semantic information for environment perception in autonomous driving. However, due to its unsteadiness in severe lighting conditions, such as sun glare, fog or heavy rain, its unreliable. On top of that, a perception module requires not only object detection in image plane but also in 3D coordinate system, which is challenging for camera. Similarly, its counterpart 3D perception sensor LiDAR is saddled with its drawbacks of visible light and expensive production costs.

Radar presents a cost-effective alternative to LiDAR as a 3D perception sensor to support camera. Radar is reliable in all weather conditions as it uses radio waves propagating through rain and fog [2], though with signal attenuation. Frequency Modulated Continuous Wave (FMCW) radar, which operates in the frequency range 77-81GHz has been a bedrock for early ADAS functions such as automatic cruise control (ACC) and automatic emergency braking (AEB).

The FMCW radar transmitted signal frequency is a linear ramp signal and the reflected signal is of the same shape (the receiver noise added on top) with some damping and phase difference due to the distance between an object and radar sensor. The received FMCW signal is further mixed with the transmitted signal to obtain an intermediate frequency (IF). The beat frequency of this signal is related to the delay which is directly proportional to the range. Similarly, phase difference across multiple chirps (Frames) allows object velocity estimation [3]. Finally, the use of multiple transmitter/receiver antennas enables estimating azimuth and/or elevation of the objects [4]. In essence, the radar signatures across (samples, chirps and transmitter/receiver antennas) are processed via fast Fourier transform (FFT) to yield a 4D cube (range, Doppler and angles). In this paper we restrict ourselves to only range, Doppler and azimuth angle estimation (3D data cube), due to the restriction in the availability of reliable dataset.

Traditionally these tensors are processed through Constant False Alarm Rate CFAR [5] algorithm to get a sparse point cloud. These points are further clustered (e.g., using DBSCAN [6]) and associated with an object. This processing ignores the intrinsic radar features, hence the only the objects having sufficiently high signal to noise Ratio (SNR) maps are detected. This hinders the detection of objects having low radar cross-section (RCS). For the purpose of improving higher detection rates, while keeping the false alarms low, recently many researchers have explored machine learning approaches [7]–[9]. For instance, the authors in [7] present a classification of airborne targets based on a supervised machine learning algorithm (SVM and Naive Bayes).

Getting intuition from computer vision community, radar researchers have also employed Convolutional Neural Network (CNN)-based networks for detection, recognition, human activity classification and path prediction [10]–[14]. Yet, these works have not fully realized the potential of Doppler signatures and rarely discussed the attention-based feature fusion. On top of it, utilizing radar as a range determination sensor, for other purposes such as heading forecasting alongside object detection has not been covered thoroughly. In this work, we consider the neural network proposed in [15] as our baseline for fusing all three radar channels. However, this baseline is further improved by the proposed cross-attention mechanism and center-offset integration in the cost function reformulation. Furthermore, we improve the ground-truth representation using the bivariate norm for the open-sourced dataset CARRADA [16]. Moreover, heading estimation is achieved by directly using stacked radar maps. For the readers'

¹The authors are with the Elektronische Fahrwerksysteme GmbH, 85080 Gaimersheim, Germany {ravi.kothari, ali.kariminezhad, christian5.mayr}@efs-auto.de

²The authors are with Institute of Automatic Control, RWTH Aachen University, Campus-Boulevard 30, 52074 Aachen, Germany h.zhang@irt.rwth-aachen.de

convenience we shortlist Our main contributions below.

- 1) Cross attention based fusion. This eliminates the need for Doppler feature replication.
- 2) Novel ground truth representation for unbiased detection.
- 3) Center offset loss, which has reduced distance error.
- 4) End to end heading estimation framework, by skipping object tracking.

The paper is organised as follows, in section II the latest radar networks are presented. Followed by the section III, where we discuss the the chosen dataset and its subsequent processing. In section IV the network architecture is setup and in section V it is compared with the state-of-the-art models. Finally section VI is dedicated for conclusion and future scope of DNN based radar detection.

II. RELATED WORKS

Considerable works using data-driven approaches for radar detection demonstrates its capability as a robust supporting sensor, in case of camera failure [15], [17]–[23]. These works use different aspects of radar and process them with various NN models. The authors in [18] use Short Time Fourier Transform (STFT) heat maps as the input to the convolution neural network CNN to classify human activities. They have utilized the fact that each dynamic objects have a unique Doppler signature which is related to its movement, geometry and size. Moreover, the authors in [17] use range-Doppler maps as the input. Their CNN network was a classifier with 3 classes (pedestrian, cyclist and car). They achieved test accuracy of 97%, demonstrating the importance of micro-Doppler signatures in classification. However, the above-mentioned methods only focus on classification tasks, that assume a single object environment, thus not applicable to the complex driving scenarios.

The authors in [24] have shown a Deep Neural Network (DNN) based radar detection using a two-stage network, where a region of interest (ROI) is selected and further processed through a classifier. It's an attempt at DNN based semantic segmentation of a 3D point cloud. The presence of ROI module and dependence on CFAR still restricts the full potential of the detector.

2D bounding box has been a linchpin for the image-based detectors, using a similar approach, [21] has applied single stage detector you only look once (YOLO) [25] on range-Doppler maps. To feed the 3D radar power spectrum into 2D YOLO network, [21] condenses the angular domain by choosing the maximum. The range-angle domain is the main perspective to observe the object RCS, hence condensing angular domain is not the best choice. On the same note [23] have used a resnet [26] backbone. The dependency on sufficiently high RCS in range-angle maps confines this approach to vehicle detection scenarios.

Furthermore, the low angular resolution makes it difficult to manually annotate the radar dataset, hence a LiDAR/camera is needed to form the bounding box. To resolve this problem [15] introduced a probabilistic map, which uses the target

peaks to create Gaussian representation. This approach leads to a stable training process and circumvents the need for box annotation [27]. Even though [15] incorporates temporal frames it fails to fuse Doppler features, hence the vulnerable road users (VRU) detection is barred to close ranges.

The authors in [22] made the first attempt at utilizing Doppler signatures with range-angle maps. This work introduces using Convolution-deconvolution (CDC) network, in which an encoder type was used to extract relevant feature maps, which are further passed through a decoder. The model is tested on vehicle detection in highway scenario relying mainly on recognizing the energy distribution of the range and angle dimension, i.e., the contribution of Doppler dimension to object detection is neglected. The authors in [19] introduced a Range-Angle-Doppler (RAD) fusion network for the purpose of semantic segmentation. Notice that, semantics are important in categorising a scene but they lack the object location, which is critical in scene understanding. The work in [20] is an extension of [15], as it utilizes all the three maps and fuses them with replicates of mean Doppler tensors. In that work, a Gaussian map is used as ground truth representation with an inception module for processing the concatenated features. Moreover, adoption of an additional skip loss function for better utilization of Doppler branch indicates this network architecture limitations in extracting Doppler.

For precise environment representation, an object's state should contain not only its location but its dynamic state, e.g., velocity and heading, too. Traditionally, object detection is first aggregated over multiple frames and then are associated and tracked for calculating heading. The authors in [28] and [29], have tried some form of heading estimation using camera images. As of now, radar community has not explored the single-stage heading estimation. Therefore, in this work we extend the detection network for further motion prediction purposes.

III. DATASET

Benchmark radar datasets such as nuScenes [30], Oxford robocar [31] and astyx [32] are all based on 3D sparse point clouds, which ignores the relevant feature maps. As raw radar data processing for enhance object detection is an emerging topic, there is a lack of corresponding radar dataset. Besides, combined with the difficulty in data interpretation, radar dataset requires additional annotation sensors for ground truth acquisition.

CRUW [15] is the first dataset delivering range-angle FFT maps, however as of writing this paper CRUW Doppler maps were not made publicly available. CARRADA [19] dataset contains synchronised camera and radar data. The authors of CARRADA have provided annotations for range, angle and Doppler maps with corresponding bounding box, sparse point and dense masks. CARRADA dataset is utilized for this work as it is the only available complete radar raw dataset. This dataset includes three classes namely pedestrians, cyclists and cars. The authors of CARRADA have also suggested the use

of this dataset for temporal predictions, which conforms with our goal for object orientation estimation.

As stated earlier, CARRADA has a machine-generated annotation. It means, the authors have used object detection and tracking with camera and this camera-based detection is projected on radar plane to get the annotation for radar raw data. Since, these annotations are not completely reliable, here we will discuss the problems confronted for improving the dataset by appropriate pre-processing. Furthermore, we will elaborate the conversion of box annotation to Gaussian one and finally, we will discuss how the orientation annotation is established.

A. Dataset Pre-Processing

Due to the error in camera calibration and the fact that radar reflection does not correspond to the boundary of an object. There are multiple examples where the box was not bounding the complete signal. Mis-annotation leads to sub-optimal network, hence, efficient data pre-processing places a crucial role in the final network performance. To compensate for these bounding box positions, the dataset was passed through a basic max-finding filter.

Granted the absence of LiDAR for ground truth annotation, the camera has eventually missed some objects at far away distance. Especially VRUs in snowy winters which also supports the axiom that visible light-based sensors struggle in bad weather. These frames with missing objects are manually identified and annotated by tracking on previous frames or by using Doppler signatures.

CARRADA dataset was meant for object detection or semantic segmentation. The heading ground truth is computed by finding the object position in multiple frames. These points are joined via a spine and the orientation is the differentiation of the spine at each instance.

B. Bivariate Norm

As stated earlier, radar signature of an object is dependent on many parameters, e.g., material, geometry and location. Hence, ground truth representation should be adaptable, such that a weak RA-RCS object, e.g., a pedestrian, should have smaller variance as compared to a high SNR signal, e.g., signal reflected from a metallic object with big cross-section, a car. This mapping will assure that the network is punished as per the signal strength. To achieve this, the authors in [15] use Gaussian-based labeling with multiple hyper-parameters that control the ground truth variance based on range, angle and object class. Besides its advantages, this method requires the overhead of tuning Gaussian covariance hyper-parameters.

To move away from manually choosing Gaussian covariance we propose the extraction of the relevant parameters of the given bounding box and map it onto the ground truth. This process guarantees that the ground truth accurately reflects the original signal without using any extra parameters. This can be interpreted as a combination of semantic segmentation and Gaussian representation. Below are the steps showing the bivariate norm mapping process:

- 1) Normalise the bounding box map by its max bin, i.e., in range 0-1.
- 2) Highlight the signal by masking with a threshold of 0.1
- 3) Find the covariance and center of the resultant masked bins
- 4) Project the bivariate norm as the ground truth using the calculated covariance and center values

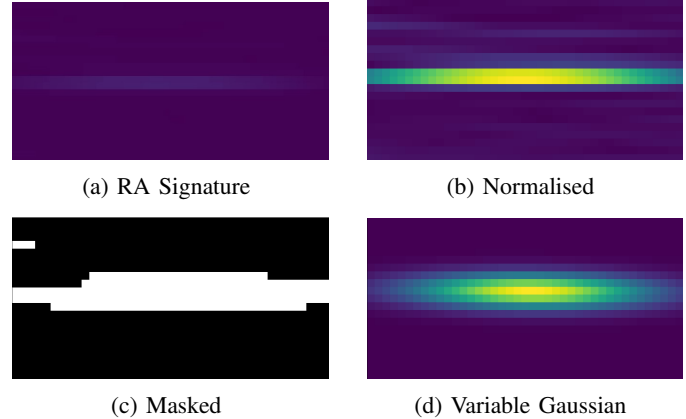


Fig. 1: Bivariate formation

For a given range μ_r and angle μ_a coordinates with covariance Σ , eq. 1 on top of the next page gives the Gaussian map. For baseline network we have considered correlation ρ to be zero and the range and angle variances are assumed to be equal.

IV. NETWORK ARCHITECTURE

Compared to image-based detection which needs to be generalized over size, frame rotation, brightness, the radar signatures are localized. Hence, the developed network is not required to correlate large features, i.e, include correlation from distant grids. As the aim is to detect objects in range-angle (RA) coordinates, the output will be of a similar shape as the input RA map. In This regard, most of the past works have been inspired by the work in medical imaging (semantic segmentation), denoising networks or by some form of image BBox (Bounding Box) detectors. The authors in [33] proposed a U-Net derived FCN (Fully Connected Network) for radar detection. The network input uses 32 concatenated range-Doppler maps estimating the objectness score of a target along with its angular position. This collective data approach termed as raw fusion becomes memory-intense in case of a larger range-Doppler maps or for the case that the past frames are exploited as multiple input channels. The authors of [?] has tried a similar approach with Doppler signatures. The authors presented their work with YOLO and Tiny YOLO [25]. The main drawback of these bounding box type detectors is to find an equivalent ground truth for radar, since radar maps do not directly provide the accurate boundary of objects.

Convolution-deconvolution (CDC) type backbones are the simplest networks for transforming data into the same space. Consequently, these CDCs are efficient and have a low

$$f(r, a) = \frac{1}{2\pi\sigma_r\sigma_a\sqrt{1-\rho^2}} \exp\left(-\frac{1}{2(1-\rho^2)}\left[\left(\frac{r-\mu_r}{\sigma_r}\right)^2 - 2\rho\left(\frac{r-\mu_r}{\sigma_r}\right)\left(\frac{a-\mu_a}{\sigma_a}\right) + \left(\frac{a-\mu_a}{\sigma_a}\right)^2\right]\right) \quad (1)$$

memory footprint. The work [34] is based on CDC network for BBox detection, similarly [15] uses CDC to estimate object probability with Gaussian maps. The model was further evaluated on CRUW [15] dataset, and it performed with 78% average recall which depicts the effectiveness of CDC. Ergo our network will be based on a CDC backbone, derived from ROD-Net [15].

A. Fusion

The initial radar and ML research [18], [35] adopted Doppler data to classify objects. Every dynamic object has its unique Doppler signature which varies with its movement, class and orientation. Considering that the Doppler lies in different space as range and angle, researchers in [19], [20], [22], have attempted feature fusion on raw radar data level. Moreover, the authors in [19] proposed a multi-view radar semantic segmentation known as MV Net. They concatenated the feature maps from range-angle (RA), angle-Doppler (AD) and range-Doppler (RD) encoders respectively, which is further processed by the decoders. Along with the fusion they have adopted ASPP (Atrous Spatial Pyramid Pooling), for using multiple scale filters, simultaneously. The authors from [22] demonstrated the use of intermediate fusion by using range, angle and Doppler encoders. This consists of an encoder-decoder with skip connections backbone. As range-angle-Doppler (RAD) maps are derived from the same 3D FFT matrix, the original matrix is first compressed by passing individual maps with encoders. Then, the features are further replicated in the missing dimension. This approach leads to a lighter decoder.

The work proposing RAMP network [20] also applied fusion for detecting Gaussian type radar objects. The authors used an auto-encoder CNN backbone with a custom loss function. Before fusion, the Doppler maps are condensed, i.e., by getting the mean across relevant axis and replicating them. Thus, transforming Doppler maps to RA plane. Moreover, the authors designed the CDC network and the late fusion on the principle of denoising RAD maps. The concatenated feature maps are further processed with a CNN header known as the inception module.

The incompatible signature of Doppler and its dissimilar map size, have driven the fusion approach to convert Doppler to range angle maps. This in turn makes the network more reliant on RA maps. Hence these models struggle with VRUs with low RCS, such as pedestrians in snow or a cyclist at long distances. To realise the full potential of Doppler signature, we introduce a novel cross attention module.

In fig 2 the target is in snow environment, hence it is difficult to detect objects by using RA map alone. Whereas one can observe, when complementary RD and AD maps are multiplied, they highlight the object location. The output mask

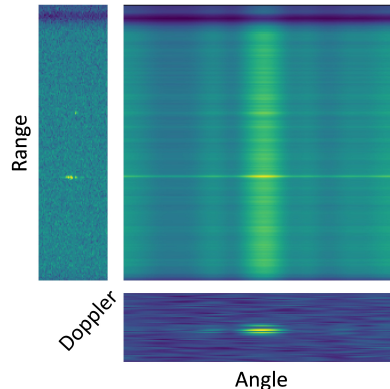


Fig. 2: Conversion of a Doppler signature to RA map

acts as a filter for dynamic objects. Our fusion module works on the same principle. We multiply the features from Doppler maps and take a softmax across the channels, thus obtaining an attention block. The resultant map could attend to the RA feature map. There is also an additional skip connection, which guarantees that the network functions even with stationary objects. This approach is inspired by transformer self-attention [36], where one can imagine **query** and **key** coming from the Doppler maps and RA features as the **value**.

Given an intermediate feature map $F \in R^{C \times H \times W}$ as input, the generalized self-attention can be written as:

$$W(F) = \alpha(F) \cdot F, \quad (2)$$

where $\alpha(\cdot)$ is an attention function

$$F' = F_{RD} \otimes F_{AD}, \quad (3)$$

where \otimes denotes element-wise multiplication.

$$F'' = \|\text{softmax}(F') \otimes F_{RA} + F_{RA}\|_{\text{layernorm}}, \quad (4)$$

where the resulting F'' will pass to the decoder.

B. Metrics

After receiving the Gaussian maps from the network, it passes through a peak detector. We use a kernel of 5×5 in a max pool layer, using this inbuilt kernel we can use the parallel computation from CUDA. The kernel size was decided after multiple experiments and by considering the minimum Gaussian size. If the detected max lies on the center of the kernel and has a confidence score of more than 0.2, it is considered as a peak. Finally, these peak coordinates alongside their intensity values pass through Distance based Non-max suppression (DNMS) module to remove false positive detection. This approach uses similar NMS algorithm

from image-based detectors, where the Intersection over Union (IOU) threshold is switched with distance among peak pairs. In this work, the mean Average Precision (mAP) is set to 2m threshold. This value represents the minimum center distance between two objects in CARRADA [19] dataset.

C. Center Offset

Observing that the network output is a rough estimate of ground truth Gaussian, it was noticed that the peaks associated with the ground truth were still a bit far away. Hence, these multiple detections increased false-positive rate as DNMS was not able to weed them out. To assist the network in improving the distance error from the ground truth, we introduced a novel center offset patch. This is a $2 \times 9 \times 9$ patch consisting of peak coordinates offset in terms of range and angle. This way, all the peaks detected before DNMS are first shifted after referencing from their respective range and angle offset maps. This has reduced the mean distance error between the associated predictions and the ground truth. The value in the bin is an indication of actual GT distance in terms of pixel. Furthermore, the maps are normalised before feeding to the network. It is important to notice that, the patch size is based on the Gaussian spread and the DNMS threshold distance.

D. Orientation

As images do not directly provide the object location, depth feature extraction requires intricate network blocks. In the case of radar, the RA maps inherently contain the localisation data, hence the network does not need multiple temporal encoders for determining object heading. In this paper, we have attempted in estimating object heading by using the concatenated RAD past frames. The heading angle ground truth is embedded in $\sin(\theta)$ and $\cos(\theta)$ maps. Due to their complementary nature, together it can cover the range -180° to $+180^\circ$.

E. Architecture

The final proposed network uses the encoder from RAMP [20] as the baseline. It consists of 6 encoder down-sampling layers and 4 layers of transpose convolutions for up-sampling. Each layer consists of PReLU [37] activation and batch normalization [38]. For detection comparison, we have used single frame RAD map. Moreover, for incorporating orientation estimation the same encoder’s first layer is adapted to use five channels. Cross attention based fusion is implemented alongside and multiple header decoder is considered for bivariate norm, center offset, orientation maps, respectively.

V. EVALUATION

In this section, we present the loss function followed by the evaluation results and its analysis. Furthermore, the baseline is compared with the proposed network. After dataset pre-processing, almost 9000 instances are delivered, these are further split into train, validate and test datasets (70%,20%,10%). The size of a RA map is 256×256 , AD map is 64×256 and RD map is 256×64 . For better generalisation, angle axis flip

and Gaussian noise are used as data augmentation. The output consists of Gaussian maps $Classes \times 256 \times 256$, center offset $2 \times 256 \times 256$, orientation maps $3 \times 256 \times 256$.

A. Loss Function

Bivariate norm is trained with focal loss L_{Bivar} . Moreover, center offset L_{center} uses focal loss too but only where the patch is present. Similarly, on orientation (L_{orien}) and velocity maps L_{velo} MSE is applied. Final loss incorporates weighted individual losses. These weights are further optimized with hyper parameter tuning process.

$$L_{total} = w_1 L_{Bivar} + w_2 L_{center} + w_3 (L_{orien} + L_{velo}) \quad (5)$$

B. Baseline

We compare our Bivariate Cross Attention network with RAMP [20]. To highlight the effectiveness of fusion module in integrating Doppler information, we also compare RODNet [15] which only uses RA maps. As the baseline networks are not implemented in CARRADA dataset, we train them from scratch. The training and validation protocol is same for baseline and proposed network.

C. Implementation

PyTorch 1.9.0 framework is utilized for training and validation. All the experiments were run on a Nvidia Quadro RTX 8000 GPU. For the baseline we have used the fixed Gaussian as the ground truth, where as the proposed network relies on bivariate norm. Batch size of 16 is used, with an initial learning rate of $1e-4$, its further reduced with plateau (factor=0.1, patience=4). Adam [39] is used as an optimizer. 80 epochs were found to be sufficient where the evaluation losses were achieving the minima. We use multiple checkpoints for saving model weights based on different criterion’s (minimum mAP, minimum validation loss and last session weights).

D. Results

Network	mAP@ 2m				Para.
	Pedes.	Cyclist	Car	Overall	
RODNet [15]	88%	84%	93%	88%	4.6 M
RAMP [20]	89%	86%	93%	89%	14.23 M
Cross Atten.	92%	85%	96%	91%	11.05 M
Bivar Cross Atten.	91%	93%	97%	94%	11.05 M

TABLE I: Performance and complexity comparison

Cyclists and pedestrians are generally one of the most difficult objects to detect due to their low RCS. For the baseline, the average precision (AP) corresponding to car is the highest at 93% proving the importance of high radar reflection for better detection. One can observe, the baseline fusion has improved the mAP by a lone 1%, this shows the ineffectiveness of the fusion network to use Doppler information. This could be attributed to the late fusion strategy and the extensive attention of the network on RA map instead of Doppler.

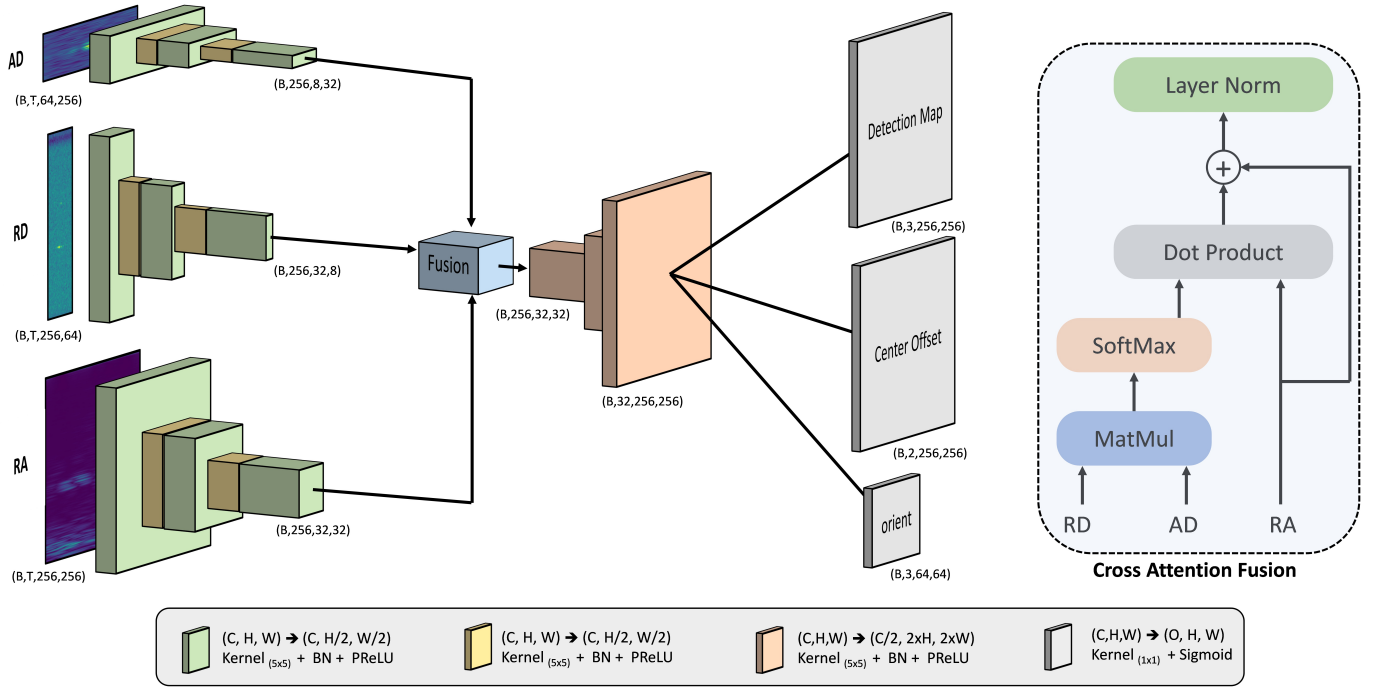


Fig. 3: Bivariate Cross Attention Network

To verify the contribution of bivariate norm, we also show the cross attention network trained with plain Gaussian. Note how the mAP from car and pedestrian have increased by 3% each. This shows the cross attention is capturing the micro-Doppler signatures. Due to a single decoder, the number of parameters has also decreased by 23% as compared to baseline.

The impact of bivariate could be seen in the Cyclist AP, it has improved the AP by 8%. This approach shows the importance of ground truth representation on network output. When comparing the base fusion network, it could be seen that the proposed network has overall improved by 5% mAP, along with better detection in all the classes. The significance of center offset maps could be depicted with the mse distance error comparison, the proposed network (0.12m) has 20% reduced error with respect to baseline (0.15m). The use of Doppler has also restricted the miss-classification below 1%, proving that the network doesn't heavily rely on RA maps signatures.

E. Orientation Estimation

By utilizing the cross attention network and incorporating past frames our network is able to detect the object heading. We report the network accuracy in $\pm 45^\circ$, $\pm 22.5^\circ$ and $\pm 11.25^\circ$ regions. These thresholds are based on the fact that a scenario understanding module requires the VRUs heading at least to a quarter region. Based on CARRADA [19] dataset, it is observed that an average human stride (1 second) takes 5 radar frames. Hence it is taken as the max number of frames that the model requires for estimating object heading. An ablation study is also done to investigate

the impact of past frames, namely 5, 3, 1 on the accuracy of object orientation estimation.

Frames	Accuracy		
	$\pm 45^\circ$	$\pm 22.5^\circ$	$\pm 11.25^\circ$
1	71%	35%	54%
3	85%	67%	42%
5	91%	77%	50%

TABLE II: Accuracy comparison of the network, while considering multiple past frames for orientation estimation

Incorporating past frames have also improved the mAP to 95%. This increased prediction confidence could be attributed to the fact that the SNR improves with more frames. Table II gives the absolute angular error between ground truth and predicted orientation. Just by stacking the past frames, we are able to achieve 50% accuracy with an error of $\pm 11.25^\circ$. As the number of frames increases the accuracy drastically goes up, which suggests the network is able to effectively fuse the maps in temporal space. Fig 4 shows the result of a 5 frame network. This example highlights the importance of radar in detecting occluded objects, due to multipath reflection. Furthermore, the network is capable of heading estimation of VRUs at long ranges. Interestingly, the single-frame network has also accuracy of 71% for $\pm 45^\circ$, which demonstrates the richness of raw radar data and the potential of DNN in extracting these information.

VI. CONCLUSION

In this paper, we have improved the radar-based object detection from range-angle-Doppler raw data. In this regard, we contributed to both data pre-processing and optimized

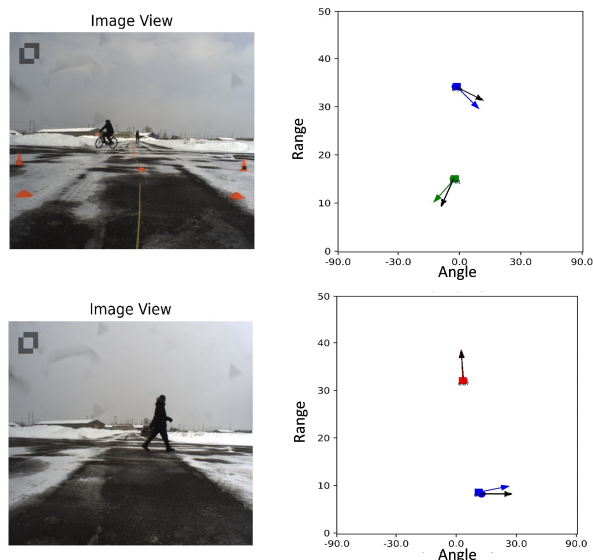


Fig. 4: Heading estimation and object detection using 5 past frames as input. The Black arrow indicates the ground truth heading and the colored arrow is the predicted heading. The colors are assigned on class basis (Pedestrian - blue, Cyclist - green, Car - red)

network design. In the pre-processing phase, the objects are labeled via class-dependant covariance Gaussian masks, deduced from the dataset. For optimizing the network, an extra feature map known as center offset feature map is exploited, which compensates for the disordered behavior of max-finding filter. This results in an overall mean average precision improvement of 5% compared to the state-of-the-art results. Moreover, we have generalized the proposed network for object orientation estimation, which eventually extracts the heading information from range-angle-Doppler raw data. This is the first work in this direction, according to the authors best knowledge.

REFERENCES

- [1] Canals, "Cars in Europe sold with level 2 autonomy driving Features," <https://www.canalys.com/>, 2019, online; accessed 27 December 2021.
- [2] Y. Golovachev, A. Etinger, G. Pinhasi, and Y. Pinhasi, "Millimeter wave high resolution radar accuracy in fog conditions-theory and experimental verification," *Sensors*, vol. 18, 07 2018.
- [3] C. Iovescu and S. Rao, "The fundamentals of millimeter wave sensors," 2017.
- [4] J. Li, R. Blum, P. Stoica, A. Haimovich, and M. Wicks, "Introduction to the issue on mimo radar and its applications," *Selected Topics in Signal Processing, IEEE Journal of*, vol. 4, pp. 2 – 4, 03 2010.
- [5] D. Abel, *Regelungstechnik*, 1st ed. Pearson, 1991.
- [6] M. Ester, H.-P. Kriegel, J. Sander, and X. Xu, "A density-based algorithm for discovering clusters in large spatial databases with noise," in *KDD*, 1996.
- [7] A. Rathi, D. Deb, N. S. Babu, and R. Mamgain, "Two-level classification of radar targets using machine learning," in *In Smart Trends in Computing and Communications*, 2019.
- [8] C. Abeynayake, V. Son, H. I. Shovon, and H. Yokohama, "Machine learning based automatic target recognition algorithm applicable to ground penetrating radar data," in *Detection and Sensing of Mines, Explosive Objects, and Obscured Targets XXIV*, 2019, pp. 1 101 202–1 101 202–17.
- [9] E. Carrera, F. Lara, M. Ortiz, A. F. Tinoco-S, and R. Leon, "Target detection using radar processors based on machine learning," 10 2020, pp. 1–5.
- [10] P. Cao, W. Xia, M. Ye, J. Zhang, and J. Zhou, "Radar-id: Human identification based on radar micro-doppler signatures using deep convolutional neural networks," *IET Radar, Sonar and Navigation*, vol. 12, pp. 729–738, 2018.
- [11] A. Angelov, A. Robertson, R. Murray-Smith, and F. Fioranelli, "Practical classification of different moving targets using automotive radar and deep neural networks," *IET Radar, Sonar and Navigation*, vol. 12, pp. 1082–1089, 04 2018.
- [12] J. Kwon and N. Kwak, "Human detection by neural networks using a low-cost short-range doppler radar sensor," in *2017 IEEE Radar Conference (RadarConf)*, 2017, pp. 0755–0760.
- [13] A. Danzer, T. Griebel, M. Bach, and K. Dietmayer, "2d car detection in radar data with pointnets," *2019 IEEE Intelligent Transportation Systems Conference (ITSC)*, Oct 2019.
- [14] R. Nabati and H. Qi, "Rrpn: Radar region proposal network for object detection in autonomous vehicles," *2019 IEEE International Conference on Image Processing (ICIP)*, Sep 2019.
- [15] Y. Wang, Z. Jiang, X. Gao, J.-N. Hwang, G. Xing, and H. Liu, "Rodnet: Radar object detection using cross-modal supervision," in *Proceedings of the IEEE/CVF Winter Conference on Applications of Computer Vision (WACV)*, January 2021, pp. 504–513.
- [16] A. Ouaknine, A. Newson, J. Rebut, F. Tupin, and P. Pérez, "Carrada dataset: Camera and automotive radar with range- angle- doppler annotations," in *2020 25th International Conference on Pattern Recognition (ICPR)*, 2021, pp. 5068–5075.
- [17] R. Pérez, F. Schubert, R. Rasshofer, and E. Biebl, "Single-frame vulnerable road users classification with a 77 ghz fmcw radar sensor and a convolutional neural network," in *2018 19th International Radar Symposium (IRS)*, 2018, pp. 1–10.
- [18] Y. Kim and T. Moon, "Human detection and activity classification based on micro-doppler signatures using deep convolutional neural networks," *IEEE Geoscience and Remote Sensing Letters*, vol. 13, no. 1, pp. 8–12, 2016.
- [19] A. Ouaknine, A. Newson, P. Pérez, F. Tupin, and J. Rebut, "Multi-view radar semantic segmentation," in *Proceedings of the IEEE/CVF International Conference on Computer Vision (ICCV)*, October 2021, pp. 15 671–15 680.
- [20] X. Gao, G. Xing, and H. Liu, "Ramp-cnn: A novel neural network for enhanced automotive radar object recognition," *IEEE Sensors Journal*, vol. PP, pp. 1–1, 11 2020.
- [21] R. Pérez, F. Schubert, R. Rasshofer, and E. Biebl, "Deep learning radar object detection and classification for urban automotive scenarios," in *2019 Kleinheubach Conference*, 2019, pp. 1–4.
- [22] B. Major, D. Fontijne, A. Ansari, R. T. Sukhvasi, R. Gowaikar, M. Hamilton, S. Lee, S. Grzechnik, and S. Subramanian, "Vehicle detection with automotive radar using deep learning on range-azimuth-doppler tensors," in *2019 IEEE/CVF International Conference on Computer Vision Workshop (ICCVW)*, 2019, pp. 924–932.
- [23] X. Dong, P. Wang, P. Zhang, and L. Liu, "Probabilistic oriented object detection in automotive radar," 06 2020, pp. 458–467.
- [24] A. Palffy, J. Dong, J. F. P. Kooij, and D. M. Gavrila, "Cnn based road user detection using the 3d radar cube," *IEEE Robotics and Automation Letters*, vol. 5, no. 2, p. 1263–1270, Apr 2020.
- [25] J. Redmon, S. Kumar Divvala, R. B. Girshick, and A. Farhadi, "You only look once: Unified, real-time object detection," *CoRR*, vol. abs/1506.02640, 2015.
- [26] K. He, X. Zhang, S. Ren, and J. Sun, "Deep residual learning for image recognition," 06 2016, pp. 770–778.
- [27] X. Zhou, D. Wang, and P. Krähenbühl, "Objects as points," in *arXiv preprint arXiv:1904.07850*, 2019.
- [28] Y. Xiang, T. Schmidt, V. Narayanan, and D. Fox, "Posecnn: A convolutional neural network for 6d object pose estimation in cluttered scenes," 2018.
- [29] M. Simon, S. Milz, K. Amende, and H.-M. Gross, "Complex-yolo: An euler-region-proposal for real-time 3d object detection on point clouds," in *Computer Vision – ECCV 2018 Workshops*, L. Leal-Taixé and S. Roth, Eds. Cham: Springer International Publishing, 2019, pp. 197–209.
- [30] H. Caesar, V. Bankiti, A. H. Lang, S. Vora, V. E. Liong, Q. Xu, A. Krishnan, Y. Pan, G. Baldan, and O. Beijbom, "nuscenes: A multimodal dataset for autonomous driving," in *CVPR*, 2020.

- [31] D. Barnes, M. Gadd, P. Murcutt, P. Newman, and I. Posner, "The oxford radar robotcar dataset: A radar extension to the oxford robotcar dataset," *arXiv preprint arXiv: 1909.01300*, 2019.
- [32] M. Meyer and G. Kusch, "Automotive radar dataset for deep learning based 3d object detection," in *2019 16th European Radar Conference (EuRAD)*, Oct. 2019, pp. 129–132.
- [33] G. Zhang, H. Li, and F. Wenger, "Object detection and 3d estimation via an fmcw radar using a fully convolutional network," 05 2020, pp. 4487–4491.
- [34] X. Dong, P. Wang, P. Zhang, and L. Liu, "Probabilistic oriented object detection in automotive radar," 06 2020, pp. 458–467.
- [35] K. Patel, K. Rambach, T. Visentin, D. Rusev, M. Pfeiffer, and B. Yang, "Deep learning-based object classification on automotive radar spectra," *2019 IEEE Radar Conference (RadarConf)*, pp. 1–6, 2019.
- [36] A. Vaswani, N. Shazeer, N. Parmar, J. Uszkoreit, L. Jones, A. N. Gomez, L. u. Kaiser, and I. Polosukhin, "Attention is all you need," in *Advances in Neural Information Processing Systems*, I. Guyon, U. V. Luxburg, S. Bengio, H. Wallach, R. Fergus, S. Vishwanathan, and R. Garnett, Eds., vol. 30. Curran Associates, Inc., 2017.
- [37] K. He, X. Zhang, S. Ren, and J. Sun, "Delving deep into rectifiers: Surpassing human-level performance on imagenet classification," *CoRR*, vol. abs/1502.01852, 2015.
- [38] S. Ioffe and C. Szegedy, "Batch normalization: Accelerating deep network training by reducing internal covariate shift," in *Proceedings of the 32nd International Conference on International Conference on Machine Learning - Volume 37*, ser. ICML'15. JMLR.org, 2015, p. 448–456.
- [39] D. P. Kingma and J. Ba, "Adam: A method for stochastic optimization," in *3rd International Conference on Learning Representations, ICLR 2015, San Diego, CA, USA, May 7-9, 2015, Conference Track Proceedings*, Y. Bengio and Y. LeCun, Eds., 2015.